

Water Soluble Molecular Switches of Fluorescence Based on the Ni<sup>III</sup>/Ni<sup>II</sup> Redox ChangeLuigi Fabbrizzi,<sup>\*†</sup> Maurizio Licchelli,<sup>†</sup> Stefano Mascheroni,<sup>†</sup> Antonio Poggi,<sup>†</sup> Donatella Sacchi,<sup>†</sup> and Michele Zema<sup>‡§</sup>

Dipartimento di Chimica Generale, Università di Pavia, via Taramelli 12, I-27100 Pavia, Italy, and Centro Grandi Strumenti, Università di Pavia, via A. Bassi 21, I-27100 Pavia, Italy

Received June 27, 2002

The water soluble Ni<sup>II</sup> complexes of the cyclam derivatives with 1,3-benzodioxole and 1,2,3-trimethoxybenzene display the fluorescent emission typical of the covalently linked fluorophores, which results from a charge transfer excited state. On oxidation to Ni<sup>III</sup>, the fluorescence is completely quenched due to the occurrence of an electron transfer (eT) process from the excited fluorogenic fragment FI\* to the oxidized metal. Thus, fluorescence can be switched off/on at will, for several cycles, by consecutively oxidizing and reducing the metal center, in controlled potential electrolysis experiments both in acetonitrile and in aqueous 0.1 M HClO<sub>4</sub>. Occurrence of an eT process from FI\* to Ni<sup>III</sup> ultimately depends upon the easy oxidation of FI to FI<sup>+</sup>, whereas failure of the occurrence of an eT process from Ni<sup>II</sup> to FI\* has to be ascribed to the particular resistance of FI fragments to the reduction.

## Introduction

Fluorescence is an interesting property displayed by a limited number of molecules (fluorophores), which can be conveniently used to generate signals at the molecular level.<sup>1</sup> Signaling requires that an operator be able to modulate fluorescence from the outside by means of a given input: chemical (the variation of the concentration of a species in the solution, e.g., H<sup>+</sup>),<sup>2</sup> electrochemical (the variation of the potential of an electrode),<sup>3</sup> or thermal (the change of temperature).<sup>4</sup> The action of the operator needs to be mediated by a molecular subunit, which translates the external input into a language intelligible to the fluorophore. In the case of an electrochemical input, this subunit must be a redox active system, which, according to the value of the

potential of the working electrode, exists in either a reduced form (RED) or an oxidized form (OX).

It may happen that the subunit, when in a given state, e.g., OX, quenches the fluorophore, through either an electron transfer (eT) or an electronic energy transfer (ET) mechanism, but, when in the RED state, leaves fluorescence unperturbed. Under these circumstances, appropriate varia-

\* Author to whom correspondence should be addressed. E-mail: fabbrizz@unipv.it.

† Dipartimento di Chimica Generale, Università di Pavia.

‡ Centro Grandi Strumenti, Università di Pavia.

§ Present affiliation: Dipartimento di Scienze della Terra, Università di Pavia, via Ferrata 1, I-27100 Pavia, Italy.

(1) (a) Lehn, J.-M. *Supramolecular Chemistry. Concepts and Perspectives*; VCH: Weinheim, 1995. (b) de Silva, A. P.; Gunaratne, H. Q. N.; Gunlaugsson, T.; Huxley, A. J. M.; McCoy, C. P.; Rademacher, J. T.; Rice, T. E. *Chem Rev.* **1997**, *97*, 1515. (c) Ashton, P. R.; Ballardini, R.; Balzani, V.; Boyd, S. E.; Credi, A.; Gandolfi, M. T.; Gómez-López, M.; Iqbal, S.; Philp, D.; Preece, J. A.; Prodi, L.; Ricketts, H. G.; Stoddart, J. F.; Tolley, M. S.; Venturi, M.; White, A. J. P.; Williams, D. J. *Chem. Eur. J.* **1997**, *3*, 146. (d) Amendola, V.; Fabbrizzi, L.; Licchelli, M.; Mangano, C.; Pallavicini, P.; Parodi, L.; Poggi, A. *Coord. Chem. Rev.* **1999**, *190–192*, 649. (e) Fabbrizzi, L.; Licchelli, M.; Pallavicini, P. *Acc. Chem. Res.* **1999**, *32*, 846.

(2) (a) de Silva, A. P.; Rupasinghe, R. A. D. *J. Chem. Soc., Chem. Commun.* **1985**, 1669. (b) de Silva, A. P.; de Silva, S. A. *J. Chem. Soc., Chem. Commun.* **1986**, 1709. (c) Bissell, R. A.; de Silva, A. P.; Gunaratne, H. Q. N.; Lynch, P. L. M.; Maguire, G. E. M.; Sandanayake, K. R. A. S. *Chem. Soc. Rev.* **1992**, 187. (d) Grigg, R.; Holmes, J. M.; Jones, S. K.; Norbert, W. D. *J. Chem. Soc., Chem. Commun.* **1994**, 185. (e) de Silva, A. P.; Gunaratne, H. Q. N.; McCoy, C. P. *Chem. Commun.* **1996**, 2399. (f) de Silva, S. A.; Zavaleta, A.; Baron, D. E.; Allam, O.; Isidor, E. V.; Kashimura, N.; Percapio, J. M. *Tetrahedron Lett.* **1997**, *38*, 2237. (g) Krauss, R.; Weing, H.-G.; Seydack, M.; Bendig, J.; Koert, U. *Angew. Chem., Int. Ed.* **2000**, *39*, 1835. (h) Fabbrizzi, L.; Licchelli, M.; Rospo, C.; Sacchi, D.; Zema, M. *Inorg. Chim. Acta* **2000**, *300–302*, 453.

(3) (a) Gouille, V.; Harriman, A.; Lehn, J.-M. *J. Chem. Soc., Chem. Commun.* **1993**, 1034. (b) Otsuki, J.; Tsujino, M.; Iizaki, T.; Araki, K.; Seno, M.; Takatera, K.; Watanabe, T. *J. Am. Chem. Soc.* **1997**, *119*, 7895. (c) Arounaguiri, S.; Maiya, B. G. *Inorg. Chem.* **1999**, *38*, 842. (d) Ashton, P. R.; Balzani, V.; Becher, J.; Credi, A.; Fyfe, M. C. T.; Mattersteig, G.; Menzer, S.; Nielsen, M. B.; Raymo, F. M.; Stoddart, J. F.; Venturi, M.; Williams, D. J. *J. Am. Chem. Soc.* **1999**, *121*, 3951. (e) Balzani, V.; Credi, A.; Mattersteig, G.; Matthews, O. A.; Raymo, F. M.; Stoddart, J. F.; Venturi, M.; White, A. J. P.; Williams, D. J. *J. Org. Chem.* **2000**, *65*, 1924. (f) Zahavy, E.; Fox, M. A. *Chem. Eur. J.* **1998**, *4*, 1647. (g) Akasaka, T.; Otsuki, J.; Araki, K. *Chem. Eur. J.* **2002**, *8*, 130.

(4) Engeser, M.; Fabbrizzi, L.; Licchelli, M.; Sacchi, D. *Chem. Commun.* **1999**, 1191.

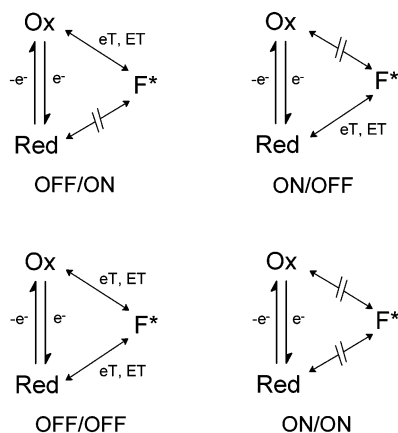
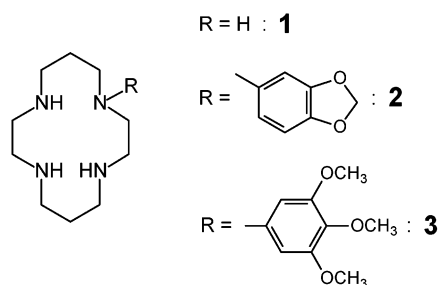


**Figure 1.** Influence of the oxidation state of the redox active subunit on the emission properties of the covalently linked fluorophore: four different situations are possible.

tions of the potential switch the state of the redox active subunit from RED to OX in a reversible fashion and, accordingly, switch fluorescence ON/OFF, in principle indefinitely. If the fluorophore and the redox active subunit are two distinct particles, fluorescence control results from a bimolecular collision, an event requiring relatively high concentrations of the colliding particles. More conveniently, the fluorophore and the redox active fragment can be covalently linked together by a short spacer: in this case, the control subunit can selectively communicate with the fluorescent moiety by means of an *intramolecular* eT or ET process, either through bond or through space. This can give rise to an efficient molecular switch of fluorescence, which operates through an electrochemical input. Switching situations are achieved when (i) the OX state quenches the fluorophore and the RED state does not (OFF/ON switch); (ii) it is the RED state that quenches the emission of the proximate fluorophore, and the OX form does not (ON/OFF switch). Unfavorable situations, for switching purposes, are those in which both states quench fluorescence (OFF/OFF) or both keep fluorescence unperturbed (ON/ON).<sup>1c,5</sup> The four situations are illustrated by the triangular schemes in Figure 1.



The redox active subunit must undergo a fast and reversible change, possibly involving one-electron stoichiometry. In this sense, transition metal complexes are ideal candidates to play the role of control subunits, as (i) they present pairs of consecutive oxidation states linked by a fast and reversible change, and (ii) the relative stability of OX and RED can be

tuned by modifying the donating tendencies of the ligand(s). We have previously shown that the Cu<sup>II</sup>/Cu<sup>I</sup> couple,<sup>6</sup> within a macrocyclic environment containing thioetheral sulfur atoms, and the Ni<sup>III</sup>/Ni<sup>II</sup> couple,<sup>7</sup> encircled by a tetramine macrocycle, can selectively control the emission of a polyaromatic fluorophore (naphthalene, anthracene) covalently linked to the ligand framework, giving rise to redox switches of fluorescence of the OFF/ON type. Due to the lipophilic nature of the fluorophore, studies could not be carried out in water, but they could be carried out in nonaqueous solvents like MeCN and alcohols. We report here two new redox switches of fluorescence based on the Ni<sup>II</sup> complexes of the macrocyclic ligands **2** and **3**, which operate through the Ni<sup>III</sup>/Ni<sup>II</sup> couple. The hosting tetramine macrocycle, which possesses the 14-membered framework of cyclam, **1**, is linked through a  $-\text{CH}_2-$  group to a fluorophore of moderately lipophilic features, which allows the corresponding Ni<sup>II</sup> and Ni<sup>III</sup> derivatives to be soluble in water. Water solubility is essential if one intends to utilize fluorescence switches in biologic fluids, in particular for estimating the redox potential of a certain environment. In this connection, it is to be noted that the potential associated with the Ni<sup>III</sup>/Ni<sup>II</sup> couple within systems **2** and **3** ranges around 1 V vs SCE.

## Experimental Section

**General Remarks.** Unless otherwise stated, commercially available reagent grade chemicals were used as purchased, without further purification. 1,4,8,11-Tetraazacyclotetradecane (cyclam, **1**) was prepared following the literature method.<sup>8</sup>

Spectrophotometric or fluorimetric grade solvents were used for spectroscopic measurements.

UV-vis spectra were recorded on a Hewlett-Packard 8452A diode array spectrophotometer; emission spectra were taken on a Perkin-Elmer LS-50B luminescence spectrometer.

Corrections for the inner filter effect<sup>9</sup> and in particular for the reabsorption of the emitted light at 315–340 nm by the nickel(III) complexes were evaluated by literature methods.<sup>9,10</sup> In all cases the corrections were lower than 5% of the observed fluorescence intensity ( $I_F$ ) values.

The relative quantum yields of fluorescence were obtained through the optically diluted method<sup>11</sup> using naphthalene ( $\Phi = 0.21$  in EtOH) as reference.<sup>12</sup>

Emission spectra at 77 K were measured in butyronitrile ( $10^{-5}$  M), by using quartz sample tubes and the same luminescence spectrometer, equipped with a Perkin-Elmer low-temperature luminescence accessory.

NMR spectra were recorded on a Bruker AMX400 spectrometer.

Mass spectra were obtained using an LCQ DECA ion trap mass spectrometer, equipped with an electrospray ionization (ESI) ion source and controlled by Xcalibur software 1.1 (Thermo-Finnigan).

- (6) De Santis, G.; Fabbrizzi, L.; Licchelli, M.; Mangano, C.; Sacchi, D. *Inorg. Chem.* **1995**, *34*, 3581.
- (7) De Santis, G.; Fabbrizzi, L.; Licchelli, M.; Sardone, N.; Velders, A. H. *Chem. Eur. J.* **1996**, *2*, 1243.
- (8) Barefield, E. K.; Wagner, F.; Herlinger, A. W.; Dahl, A. R. *Inorg. Synth.* **1975**, *16*, 220.
- (9) Lakowicz, J. R. *Principles of Fluorescence Spectroscopy*; Plenum: New York, 1983.
- (10) Credi, A.; Prodi, L. *Spectrochim. Acta, Part A* **1998**, *54*, 159.
- (11) Demas, J. N.; Crosby, G. A. *J. Phys. Chem.* **1971**, *75*, 991.
- (12) Malkin, J. *Photophysical and Photochemical Properties of Aromatic Compounds*; CRC Press: Boca Raton, FL, 1992.

(5) Bergonzi, R.; Fabbrizzi, L.; Licchelli, M.; Mangano, C. *Coord. Chem. Rev.* **1998**, *170*, 31.

Redox potential values were determined by voltammetric techniques, on a Princeton Applied Research model 273 potentiostat–galvanostat. Investigations on MeCN solutions, made 0.1 M in  $\text{Bu}_4\text{NClO}_4$ , were carried out in a conventional three-electrode cell using a platinum microsphere as a working electrode, and a silver wire as a pseudo-reference electrode which was calibrated vs the  $\text{Fc}^+/\text{Fc}$  couple used as an internal standard.<sup>13</sup> Investigations in aqueous solutions (0.1 M  $\text{HClO}_4$ ) were performed in the same cell using a glassy carbon working electrode and an SCE as reference.

CPC experiments were carried out on solutions of the nickel(II) complexes ( $1-2 \times 10^{-5}$  M) in MeCN (made 0.1 M in  $\text{Bu}_4\text{NClO}_4$ ) or in aqueous  $\text{HClO}_4$  (0.1 M), with a platinum gauze as a working electrode. The counter electrode compartment was separated from the working compartment by a U-shaped bridge filled with the same electrolyte solutions. The reference electrode was a platinum wire dipped in the working cell (its potential was calibrated through CV measurements prior to CPC) for the experiments in MeCN or an SCE for the experiments in aqueous solutions.

**SAFETY NOTE!** Perchlorate salts of metal complexes are potentially explosive and should be handled with care. In particular, they should never be heated as solids.<sup>14</sup>

**1,4,8-Tris(*tert*-butoxycarbonyl)-1,4,8,11-tetraazacyclotetradecane (triBOCCyclam), 4.** Cyclam (5 mmol, 1.0 g) was dissolved in dried dichloromethane (200 mL) and triethylamine was added (25 mmol) under a dinitrogen atmosphere. The reaction mixture was stirred, and a solution of *tert*-butoxy-dicarbonate (9 mmol) in dried dichloromethane (60 mL) was added dropwise. After the reaction mixture was cooled to  $-15^\circ\text{C}$ , another portion of *tert*-butoxy-dicarbonate (6 mmol) was added, and the mixture was stirred at room temperature overnight. The solution was treated with  $\text{Na}_2\text{CO}_3$  (0.5 N), and the organic solution was dried over  $\text{Na}_2\text{SO}_4$ . The solvent and the excess of triethylamine were removed in vacuo, and the residue was purified by liquid chromatography ( $\text{SiO}_2$ , 9:1 ethyl acetate/methanol,  $R_f$  0.5). Yield: 70.5%.  $^1\text{H NMR}$  (400 MHz,  $\text{CDCl}_3$ ):  $\delta$  3.10 (m, 12H,  $\text{CH}_2$ ), 2.70 (t, 2H,  $\text{CH}_2$ ), 2.55 (t, 2H,  $\text{CH}_2$ ), 1.86 (q, 2H,  $\text{CH}_2$ ), 1.63 (q, 2H,  $\text{CH}_2$ ), 1.38 (s, 27H,  $\text{C}(\text{CH}_3)_3$ ). MS (ESI)  $m/z$ : 501.2  $[\text{M} + \text{H}]^+$ .

**5-Bromomethyl-1,3-benzodioxole (Piperonyl Bromide).** A solution of  $\text{CBr}_4$  (1.66 g, 5 mmol) and  $\text{Ph}_3\text{P}$  (1.31 g, 5 mmol) in diethyl ether (30 mL) was added to a solution of benzo[1,3]dioxole-5-methanol (piperonyl alcohol, 0.76 g, 5 mmol) in diethyl ether (30 mL). The reaction mixture was stirred at room temperature for 3 h and filtered over a sintered glass funnel. The crude product obtained after removing the solvent was purified by liquid chromatography ( $\text{SiO}_2$ , 1:1 *n*-hexane/diethyl ether,  $R_f$  0.7). Yield: 72.5%. Anal. Calcd for  $\text{C}_8\text{H}_7\text{BrO}_2$ : C, 44.68; H, 3.28. Found: C, 44.47; H, 3.21.

**1-(1,3-Benzodioxol-5-ylmethyl)-4,8,11-tris(*tert*-butoxycarbonyl)-1,4,8,11-tetraazacyclotetradecane, 5.** TriBOCCyclam (0.45 g, 0.9 mmol) was dissolved in toluene (30 mL) in a three-neck round-bottomed flask equipped with a reflux condenser, mechanical stirrer, and dropping funnel, under a dinitrogen atmosphere.  $\text{Cs}_2\text{CO}_3$  (0.29 g, 0.9 mmol) was added, and the resulting mixture was heated to reflux with vigorous stirring, as a solution of piperonyl bromide (0.2 g, 0.9 mmol) in toluene (10 mL) was dropped through the funnel. Heating and stirring were continued for 12 h, and then the mixture was cooled to room temperature and filtered to remove cesium carbonate. Toluene was distilled off and the crude product purified by liquid chromatography ( $\text{SiO}_2$ , 95:5 AcOEt/MeOH,  $R_f$  0.75). Yield: 61.3%. MS (ESI)  $m/z$ : 635.3  $[\text{M} + \text{H}]^+$ .

(13)  $E^\circ(\text{Fc}^+/\text{Fc}) = 0.425$  V vs SCE. Gennet, T.; Milner, D. F.; Weaver, M. J. *J. Phys. Chem.* **1985**, *89*, 2787.

(14) Wolsey, W. C. *J. Chem. Educ.* **1973**, *50*, A335.

**1-(1,3-Benzodioxol-5-ylmethyl)-1,4,8,11-tetraazacyclotetradecane, 2.**  $\text{CF}_3\text{COOH}$  (5 mL) was added to a solution of **5** (0.34 g, 0.54 mmol) in  $\text{CH}_2\text{Cl}_2$  (10 mL), and the resulting mixture was magnetically stirred under a dinitrogen atmosphere for 24 h. The solvent was removed in vacuo, the oily residue was treated with acidic water (0.1 M HCl, 25 mL), and the resulting solution was extracted with diethyl ether ( $2 \times 20$  mL). The aqueous layer was made alkaline by addition of NaOH and extracted with  $\text{CH}_2\text{Cl}_2$  ( $4 \times 20$  mL). The organic layer was desiccated over  $\text{Na}_2\text{SO}_4$ , and the product was obtained as a white solid after removal of the solvent. Yield: 95.8%. MS (ESI)  $m/z$ : 335.3  $[\text{M} + \text{H}]^+$ .

**1-(3,4,5-Trimethoxybenzyl)-4,8,11-tris(*tert*-butoxycarbonyl)-1,4,8,11-tetraazacyclotetradecane, 6.** A solution of triBOCCyclam (0.5 g, 1 mmol) and 3,4,5-trimethoxybenzaldehyde (0.23 g, 1.2 mmol) in MeOH (25 mL) was acidified by addition of  $\text{CH}_3\text{COOH}$  (0.15 mL) and cooled to  $0^\circ\text{C}$  under a dinitrogen atmosphere.  $\text{NaBH}_3\text{CN}$  (0.063 g, 1 mmol) was slowly added with magnetic stirring, and then the solution was allowed to return to room temperature and stirred for 48 h. Solvent was removed at the rotary evaporator and the residue dissolved in aqueous 0.1 M  $\text{Na}_2\text{CO}_3$  (50 mL). The resulting solution was extracted by  $\text{CH}_2\text{Cl}_2$  ( $3 \times 25$  mL), and the organic layer was dried over  $\text{Na}_2\text{SO}_4$ . The dichloromethane solution was filtered, the filtrate was rotary evaporated to dryness, and the resulting crude product was purified by liquid chromatography ( $\text{SiO}_2$ , 1:1 *n*-hexane/AcOEt,  $R_f$  0.2,  $R_f$  (unreacted aldehyde) 0.8). Yield: 90.5%. MS (ESI)  $m/z$ : 681.4  $[\text{M} + \text{H}]^+$ .

**1-(3,4,5-Trimethoxybenzyl)-1,4,8,11-tetraazacyclotetradecane, 3.** The macrocyclic ligand **3** was prepared from compound **6**, by the procedure described for **2**. Yield: 96.4%. MS (ESI)  $m/z$ : 381.3  $[\text{M} + \text{H}]^+$ .

**[Ni(2)](ClO<sub>4</sub>)<sub>2</sub>.** A solution of  $\text{Ni}(\text{ClO}_4)_2 \cdot 6\text{H}_2\text{O}$  (58 mg, 0.17 mmol) in MeOH (3 mL) was slowly added to a solution of **2** (60 mg, 0.16 mmol) in MeOH (5 mL) with magnetic stirring. The resulting solution was refluxed for 2 h and then cooled to room temperature. A yellow-orange precipitate, which was recovered by filtration, was obtained by slow evaporation of the solvent. Yield: 78.6%. MS (ESI)  $m/z$ : 493.1  $[\text{M} - \text{ClO}_4]^+$ , 393.1  $[\text{M} - \text{ClO}_4 - \text{HClO}_4]^+$ .

**[Ni(3)](ClO<sub>4</sub>)<sub>2</sub>.** The complex of the trimethoxybenzyl derivative was prepared under the same experimental conditions from ligand **3**. Yield: 83.8%. MS (ESI)  $m/z$ : 539.1  $[\text{M} - \text{ClO}_4]^+$ , 439.2  $[\text{M} - \text{ClO}_4 - \text{HClO}_4]^+$ .

**Crystallographic Studies.** The crystal and molecular structure of the  $[\text{Ni}^{\text{II}}(\text{L3})](\text{ClO}_4)_2$  complex has been determined by X-ray diffraction methods. Unit cell parameters and intensity data were obtained on a Philips PW1100 four-circle diffractometer at room temperature using graphite-monochromatized Mo  $\text{K}\alpha$  radiation. Calculations were performed with the WinGX-97<sup>15</sup> software. Crystal data and the most relevant parameters used in the crystallographic study are reported in Table 1, whereas important bond lengths and angles are in Table 2. Cell dimensions were determined by least-squares fitting of 48 centered reflections monitored in the range  $8.91^\circ < \theta < 15.12^\circ$ . Corrections for  $L_p$  and empirical absorption were applied.<sup>16</sup> The structure was solved by SIR92.<sup>17</sup> The non-hydrogen atoms were refined anisotropically by full-matrix least-

(15) Farrugia, L. J. *WinGX-97, An integrated system of Publicly Available Windows Programs for the Solution, Refinement and Analysis of Single-Crystal X-Ray Diffraction*; University of Glasgow: Glasgow, 1997.

(16) North, A. C. T.; Philips, D. C.; Mathews, F. S. *Acta Crystallogr.* **1968**, *A24*, 351.

(17) Altomare, A.; Cascarano, G.; Giacovazzo, C.; Gualardi, A. *J. Appl. Crystallogr.* **1993**, *26*, 343.



**Table 1.** Crystal and Refinement Data

formula	Ni <sub>4</sub> C <sub>20</sub> H <sub>36</sub> Cl <sub>2</sub> O <sub>11</sub>
fw	638.14
cryst size (mm)	0.16 × 0.21 × 0.56
cryst syst	monoclinic
space group	<i>P</i> 2 <sub>1</sub> / <i>n</i>
<i>a</i> (Å)	8.548(4)
<i>b</i> (Å)	21.255(9)
<i>c</i> (Å)	15.257(8)
β (deg)	95.001(8)
<i>V</i> (Å <sup>3</sup> )	2762(2)
<i>Z</i>	4
<i>D</i> <sub>calc</sub> (g cm <sup>-3</sup> )	1.535
<i>T</i> (K)	298(3)
μ (mm <sup>-1</sup> )	0.958
scan type	ω-2θ
θ range (deg)	2–30
abs correction meth	ψ-scan
index ranges	-12 ≤ <i>h</i> ≤ 12, -29 ≤ <i>k</i> ≤ 29, 0 ≤ <i>l</i> ≤ 21
reflns meas/unique	16381/8018 ( <i>R</i> <sub>int</sub> = 0.0708)
refinement type	<i>F</i> <sup>2</sup>
<i>R</i> 1 <sup>a</sup>	0.0619
<i>R</i> <sub>all</sub>	0.1326
<i>wR</i> 2	0.1538
GOF <sup>b</sup>	0.990
refined params	454
weighting scheme	$w = 1/[\sigma^2(F_o^2) + (0.0720P)^2]$ where $P = (F_o^2 + 2F_c^2)/3$
(shift/esd) <sub>max</sub>	0.001
max, min Δρ (e Å <sup>-3</sup> )	0.721, -0.556

<sup>a</sup>  $R1 = \sum ||F_o| - |F_c|| / \sum |F_o|$  (calculated on 4380 reflections with  $I > 2\sigma_I$ ). <sup>b</sup>  $GOF = S = [\sum [w(F_o^2 - F_c^2)^2] / (n - p)]^{0.5}$ , where *n* is the number of reflections and *p* is the total number of parameters refined.

**Table 2.** Selected Bond Distances (Å) and Angles (deg)

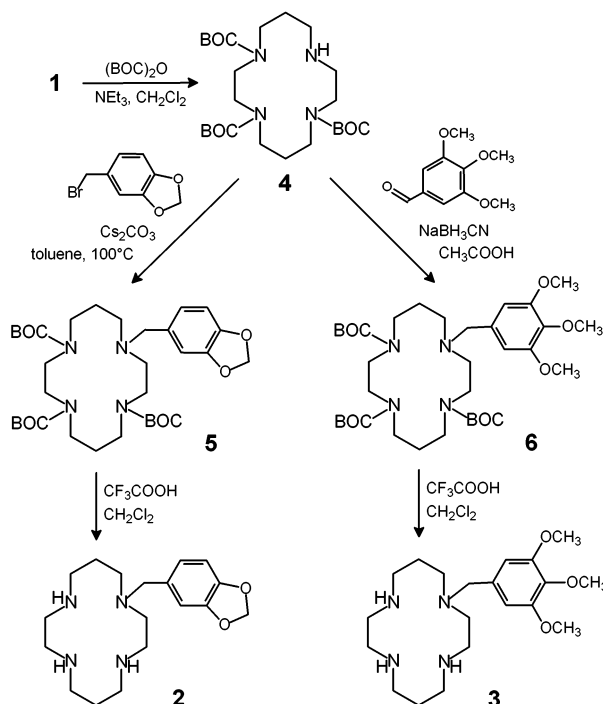
Ni1–N1	1.974(3)	Ni1–N3	1.938(3)
Ni1–N2	1.933(3)	Ni1–N4	1.933(3)
N1–Ni1–N2	87.4(1)	N1–Ni1–N3	178.0(1)
N1–Ni1–N4	91.2(1)	N2–Ni1–N3	94.6(1)
N2–Ni1–N4	176.1(1)	N3–Ni1–N4	86.8(1)

squares using SHELXL-97.<sup>18</sup> Hydrogen atoms were located in the difference Fourier maps and refined isotropically, except those bound to the methyl groups, which were inserted in the calculated positions and refined using a riding model and imposing an isotropic displacement factor proportional (× 1.5) to that of their neighboring atom. Atomic scattering factors were taken from *International Tables for X-ray Crystallography*.<sup>19</sup> Diagrams of the molecular structure were produced by the ORTEP-3 program.<sup>20</sup>

## Results and Discussion

**Syntheses and Crystallographic Studies.** Functionalized tetraaza macrocycles **2** and **3** were prepared according to the synthetic pathways reported in Scheme 1. The first step, which was common to both synthetic routes, consists of the protection with *tert*-butyloxycarbonyl (BOC) groups of three secondary amino groups of cyclam and was carried out according to a modified literature procedure.<sup>21</sup>

The fluorogenic subunits were introduced onto the macrocyclic framework by a nucleophilic substitution on piperonyl

**Scheme 1**

bromide (intermediate **5**) or by a reductive amination with trimethoxybenzaldehyde (intermediate **6**)

The use of triBOCcyclam, **4**, allows one to address functionalization reactions toward monosubstituted products. Attempts to prepare tetraazamacrocyclic **2** by direct reaction of unprotected cyclam (5-fold excess) with piperonyl bromide always afforded mixtures of polysubstituted products which could not be efficiently separated by common chromatographic methods.

Tris-BOC intermediates, **5** and **6**, were deprotected in trifluoroacetic acid by a standard procedure, affording the macrocyclic ligands **2** and **3** in almost quantitative yield.

Complexes were prepared by simply reacting each ligand with a slight excess of nickel(II) perchlorate in methanol and were isolated as yellow-orange microcrystalline products. Crystals of the [Ni<sup>II</sup>(**3**)](ClO<sub>4</sub>)<sub>2</sub> complex salt, suitable for X-ray investigations, were obtained by slow evaporation of an ethanolic solution. In the case of the [Ni<sup>II</sup>(**2**)](ClO<sub>4</sub>)<sub>2</sub>, any attempt to grow X-ray quality crystals afforded yellow-orange needles, which, however, were not of satisfactory quality for crystallographic investigations.

The molecular structure of the complex is shown in Figure 2. The tetramine macrocycle is coplanarly coordinated, according to a square geometry. In fact, the metal center lies only 0.033 Å out of the N<sub>4</sub> mean plane, and the four nitrogen atoms are displaced with respect to the plane with distances ranging from 0.025 to 0.034 Å. The Ni<sup>II</sup>–N distances, ranging over the 1.933–1.974 Å interval, are those expected for a nickel(II) ion in its low-spin state.<sup>22</sup> The two perchlorate ions are located along the axis perpendicular to the four-nitrogen plane, but the long Ni<sup>II</sup>–O distances (3.037

(18) Sheldrick, G. M. *SHELX-97, Programs for Crystal Structure Analysis*; University of Göttingen: Göttingen, Germany, 1998.

(19) *International Tables for X-ray Crystallography*, Kynoch: Birmingham, England, 1974; Vol. 4, pp 99–101 and 149–150.

(20) Farrugia, L. J. *J. Appl. Crystallogr.* **1997**, *30*, 565.

(21) Brandes, S.; Gros, C.; Denat, F.; Pullumbi, P.; Guillard, R. *Bull. Soc. Chim. Fr.* **1996**, *133*, 65.

(22) (a) Barefield, E. K.; Cheng, D.; Van Derveer, D. G. *J. Chem. Soc., Chem. Commun.* **1981**, 302. (b) Prasad, L.; Nyburg, S. C. *Acta Crystallogr.* **1987**, *C43*, 1038.

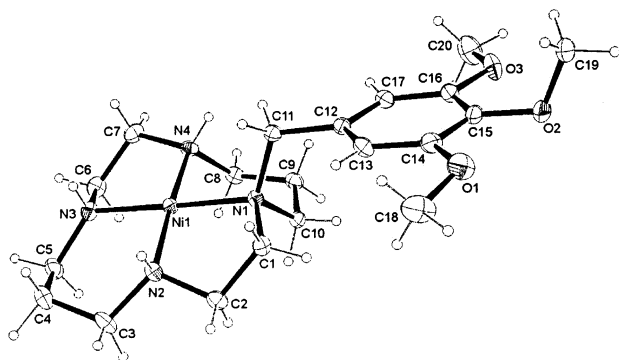


**Figure 2.** ORTEP view of the  $[\text{Ni}^{\text{II}}(\mathbf{3})]^{2+}$  complex cation.

and 3.272 Å respectively for the two ions) exclude any serious interaction of  $\text{ClO}_4^-$  with the metal. In other words, the 3,4,5-trimethoxybenzyl substituent does not seem to exert any disturbing effect on coordination. In particular, the fluorogenic fragment points outward with respect to the macrocyclic ring: as a consequence of the presence of the  $-\text{CH}_2-$  interfacing group, the  $\text{N}_4$  macrocyclic ring and the aromatic ring of the fluorophore stay on almost parallel planes (angle between the planes:  $15.9^\circ$ ).

**Solution Properties of the Nickel(II) Complexes.** The two-component systems **2** and **3** possess the framework of the symmetric 14-membered tetramine macrocycle cyclam, **1**. Among polyamine macrocycles of varying denticity and ring size, cyclam and its transition metal complexes exhibit unique properties, which derive from the ligand's ability to place its donor atoms in the positions desired by the metal centers (i.e., the corners of a square) and to establish especially strong coordinative interactions. In particular, (i) cyclam complexes are very resistant to the metal extrusion (as an example,  $[\text{Ni}^{\text{II}}(\text{cyclam})]^{2+}$ , in spite of the high basicity of the uncoordinated tetramine, persists in 1 M  $\text{HClO}_4$  with a half-life of 30 years),<sup>23</sup> and (ii) they can achieve unusually high oxidation states of the encircled metal (e.g.,  $\text{Ni}^{\text{III}}$ ,  $\text{Cu}^{\text{III}}$ ,  $\text{Ag}^{\text{II}}$ , and  $\text{Ag}^{\text{III}}$ ); this latter property is strictly related to the capability of cyclam to establish strong in-plane interactions, which raise the energy of the HOMO antibonding orbital, essentially metallic in character, from which the electron is abstracted on oxidation. For instance, the potential of the  $[\text{Ni}^{\text{III}}(\text{cyclam})]^{3+}/[\text{Ni}^{\text{II}}(\text{cyclam})]^{2+}$  couple in 1 M  $\text{HCl}$  is 0.71 V vs NHE,<sup>24</sup> something like the familiar  $[\text{Fe}^{\text{III}}(\text{H}_2\text{O})_6]^{3+}/[\text{Fe}^{\text{II}}(\text{H}_2\text{O})_6]^{2+}$  couple potential, indicating that the  $\text{Ni}^{\text{II}}$  and the  $\text{Ni}^{\text{III}}$  complex have a comparable stability and are both fairly stable in water.

In systems **2** and **3**, robust fluorophores, 1,3-benzodioxole and 1,2,3-trimethoxybenzene, were linked to one nitrogen atom of the cyclam skeleton, through a methylene group. The two fluorogenic fragments have in common a phenyl ring containing electron donor substituent(s), absorb light in the 200–300 nm interval, and emit light in the 300–350 nm interval, with a relatively high quantum yield (1,2-benzodioxole,  $\Phi = 0.31$ ; 1,2,3-trimethoxybenzene, 0.076). Absorption and emission data in MeCN for  $[\text{Ni}^{\text{II}}(\mathbf{2})]^{2+}$ ,  $[\text{Ni}^{\text{II}}(\mathbf{3})]^{2+}$ , and the plain fluorophores, used as reference compounds, are summarized in Table 3.

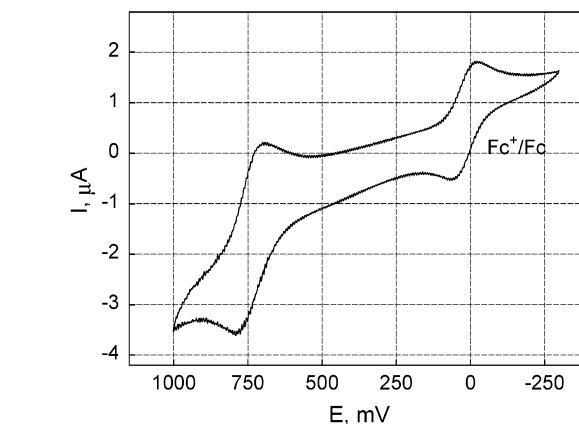


**Figure 3.** Cyclic voltammetry profile of a  $10^{-3}$  M solution of  $[\text{Ni}^{\text{II}}(\mathbf{3})]^{2+}$  in MeCN made 0.1 M in  $\text{Bu}_4\text{NClO}_4$ . Potential scale is referred to the  $\text{Fc}^+/\text{Fc}$  couple, used as internal reference.

**Table 3.** Absorption and Emission Data in MeCN for Complexes  $[\text{Ni}(\mathbf{2})]^{2+}$ ,  $[\text{Ni}(\mathbf{3})]^{2+}$ , and Reference Compounds 1,3-Benzodioxole and Trimethoxybenzene

	$\lambda_{\text{abs}}$ , nm	$\epsilon$ , $\text{M}^{-1} \text{cm}^{-1}$	$\lambda_{\text{em}} (\lambda_{\text{exc}})$ , nm	$\Phi$
1,3-benzodioxole	200 232 284	27900 4380 4100	315 (284)	0.31
$[\text{Ni}(\mathbf{2})]^{2+}$	206 236 286	23300 5140 4460	326 (286)	0.21
1,2,3-trimethoxybenzene	204 268	32300 710	310 (270)	0.076
$[\text{Ni}(\mathbf{3})]^{2+}$	208 274(sh)	28600	338 (280)	0.058

( $\mathbf{3}$ )<sup>2+</sup>, and the plain fluorophores, used as reference compounds, are summarized in Table 3.

In diluted solutions ( $10^{-5}$ – $10^{-4}$  M), nickel(II) complexes formed by cyclam derivatives **2** and **3** display electronic spectra which are very similar to those of 1,3-benzodioxole and 1,2,3-trimethoxybenzene, respectively (see  $\lambda$  and  $\epsilon$  values in Table 3). At higher concentrations ( $>10^{-3}$  M), a low-intensity band centered at 450–470 nm ( $\epsilon = 40$ – $50 \text{ M}^{-1} \text{cm}^{-1}$ ) is observed. It is typical of the nickel(II) complexes with cyclam derivatives and is ascribed to a d–d transition in a square-planar geometry.

The emission spectra of  $[\text{Ni}^{\text{II}}(\mathbf{2})]^{2+}$  and  $[\text{Ni}^{\text{II}}(\mathbf{3})]^{2+}$  exhibit broad bands (at 326 and 338 nm in MeCN, respectively), which are only slightly red-shifted (by 10–20 nm), if compared to the corresponding bands displayed by 1,2-benzodioxole and 1,2,3-trimethoxybenzene, respectively. Moreover, the fluorescence quantum yields corresponding to  $[\text{Ni}^{\text{II}}(\mathbf{2})]^{2+}$  and  $[\text{Ni}^{\text{II}}(\mathbf{3})]^{2+}$  ( $\Phi = 0.21$  and 0.058 in MeCN, respectively) are not much lower than those determined for the unsubstituted fluorophores (see Table 3).

Voltammetric studies at solid electrodes were carried out in an MeCN solution (using a platinum microsphere as a working electrode) and in water (using a glassy carbon electrode): in any case, reversible CV profiles were obtained on oxidation (see in Figure 3 the profile obtained for a solution of  $[\text{Ni}^{\text{II}}(\mathbf{3})]^{2+}$  in an MeCN solution, made 0.1 M in  $\text{Bu}_4\text{NClO}_4$ ). The measurements in water were performed in

(23) Billo, E. J. *Inorg. Chem.* **1984**, *23*, 236.

(24) Calligaris, M.; Carugo, O.; Crippa, G.; De Santis, G.; Di Casa, M.; Fabbrizzi, L.; Poggi, A.; Seghi, B. *Inorg. Chem.* **1990**, *29*, 2964.

**Table 4.** Halfwave Potential Values Related to the Ni<sup>III</sup>/Ni<sup>II</sup> Redox Exchange in MeCN and Aqueous 0.1 M HClO<sub>4</sub>

complex	$E_{1/2}(\text{Ni}^{\text{III}}/\text{Ni}^{\text{II}})$ , V vs Fc <sup>+</sup> /Fc <sup>a</sup>	$E_{1/2}(\text{Ni}^{\text{III}}/\text{Ni}^{\text{II}})$ , V vs SCE <sup>b</sup>
[Ni( <b>1</b> )] <sup>2+</sup>	0.59 <sup>c</sup>	0.75 <sup>d</sup>
[Ni( <b>2</b> )] <sup>2+</sup>	0.75	0.94
[Ni( <b>3</b> )] <sup>2+</sup>	0.73	0.93

<sup>a</sup> In MeCN 0.1 M Bu<sub>4</sub>NClO<sub>4</sub>. <sup>b</sup> In 0.1 M aqueous HClO<sub>4</sub>. <sup>c</sup> See ref 26. <sup>d</sup> In 1 M aqueous HClO<sub>4</sub>; see ref 27.

0.1 M HClO<sub>4</sub> as the stability of Ni<sup>III</sup> complexes with respect to the decomposition is distinctly enhanced in acidic solutions.<sup>25</sup>

Half-wave potential values associated with the Ni<sup>III</sup>/Ni<sup>II</sup> redox change for complexes of **1–3** are reported in Table 4. It is seen that the presence of a benzyl-like substituent on a nitrogen atom (macrocycles **2** and **3**) makes the potential moderately more positive (and the attainment of the Ni<sup>III</sup> state slightly more difficult) with respect to the corresponding complex of the unsubstituted ligand **1**, cyclam. This is a generally observed behavior and is related to the steric effects exerted by the substituent, which weaken the metal–tertiary nitrogen atom interaction;<sup>28</sup> in fact, in the [Ni<sup>II</sup>(**3**)]<sup>2+</sup> complex, the Ni<sup>II</sup>–N(tertiary) distance is slightly, but significantly, higher than the Ni<sup>II</sup>–N(secondary) distance. As a consequence of the less intense in-plane interaction, the HOMO antibonding orbital is destabilized to a lower extent and the abstraction of the electron on oxidation is less favored.

**Redox-Driven Fluorescence Switching.** Electrochemical investigations showed that Ni<sup>II</sup> and Ni<sup>III</sup> states within the cavity of macrocycles **2** and **3** are connected by a fast and reversible redox change, taking place at a not too positive half-wave potential. In order to verify the fluorescence switching behavior, we have now to demonstrate the occurrence of a selective interference of each oxidation state on the emission properties of the proximate fluorophore. This has been carried out by measuring the emission spectra in the course of controlled potential coulometry (CPC) experiments performed on both MeCN and acidic aqueous solutions of [Ni<sup>II</sup>(**2**)]<sup>2+</sup> and [Ni<sup>II</sup>(**3**)]<sup>2+</sup>.

As already mentioned, Ni<sup>II</sup> complexes (RED state) in MeCN solution display almost the same fluorescence spectra as the individual fluorogenic fragments, indicating that the divalent metal center does not seriously interfere with the nearby fluorogenic fragment. Moreover, the emission properties of the complexes in water solution do not substantially differ from those in MeCN (a direct comparison with the plain fluorophores cannot be made due to their poor solubility in water). As an example, the spectrum of the [Ni<sup>II</sup>(**2**)]<sup>2+</sup> complex in 0.1 M aqueous HClO<sub>4</sub>, prior to the electrolysis, displaying a poorly structured broad emission band centered

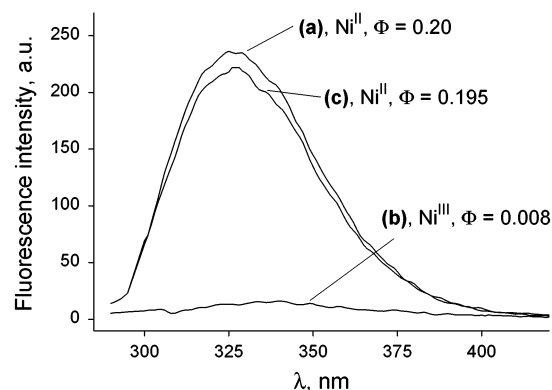


**Figure 4.** Emission spectra of [Ni<sup>II</sup>(**2**)]<sup>2+</sup>, measured during controlled potential coulometry in aqueous 0.1 M HClO<sub>4</sub>: prior to electrolysis (a); after electrolysis at 1.2 V (b); after electrolysis at 0.7 V (c).  $\lambda_{\text{exc}}$ : 286 nm.

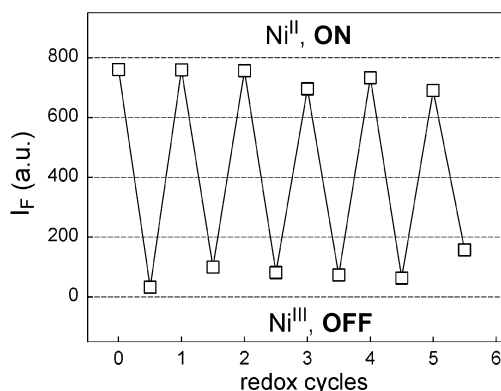


**Figure 5.** Cyclic variation of  $I_F$  (fluorescence intensity) upon consecutive oxidation/reduction processes on the [Ni<sup>II</sup>(**2**)]<sup>2+</sup> complex in aqueous 0.1 M HClO<sub>4</sub>.

at  $\lambda_{\text{max}} = 324 \text{ nm}$  ( $\Phi = 0.20$ ), is shown in Figure 4. In the CPC experiment, the potential of the working electrode (a platinum gauze) was adjusted to the potential of 1.2 V vs SCE (i.e., about 250 mV more positive than the  $E_{1/2}$  value determined by CV), in order to perform exhaustive oxidation to Ni<sup>III</sup>. The emission spectrum of the solution was measured at the end of the electrolysis experiment (after the passage of  $1.04 \pm 0.05$  electrons) showing a distinct decrease of the emission intensity ( $\Phi = 0.008$ , see Figure 4).

On the other hand, on reduction of Ni<sup>III</sup> to Ni<sup>II</sup>, performed by adjusting the potential of the working electrode to 0.7 V (i.e., about 250 mV less positive than the  $E_{1/2}$  value), the fluorescence of the solution is progressively restored: in particular, full emission ( $\Phi = 0.195$ , see Figure 4) is observed after the passage of  $1.05 \pm 0.05$  electrons, on reduction. We carried out up to five complete redox cycles without any apparent degradation of the system: in particular, about 100% of the fluorescence intensity was recovered after each reduction step (see Figure 5).

A completely similar behavior was observed for the [Ni<sup>II</sup>(**3**)]<sup>2+</sup> complex, both in MeCN and in water: the results of the CPC experiment coupled to spectrofluorimetric measurements performed on [Ni<sup>II</sup>(**3**)]<sup>2+</sup> in 0.1 M aqueous HClO<sub>4</sub> are illustrated in Figure 6.

Thus, we are in the presence of two new robust and water soluble redox switches of fluorescence.

(25) De Santis, G.; Fabbrizzi, L.; Poggi, A.; Taglietti, A. *Inorg. Chem.* **1994**, *33*, 134.

(26) Abbà, F.; De Santis, G.; Fabbrizzi, L.; Licchelli, M.; Manotti Lanfredi, A. M.; Pallavicini, P.; Poggi, A.; Ugozzoli, F. *Inorg. Chem.* **1994**, *33*, 1366.

(27) 1 M aqueous HClO<sub>4</sub>. Pallavicini, P.; Perotti, A.; Poggi, A.; Seghi, B.; Fabbrizzi, L. *J. Am. Chem. Soc.* **1987**, *109*, 5139.

(28) Ciampolini, M.; Fabbrizzi, L.; Licchelli, M.; Perotti, A.; Pezzini, F.; Poggi, A. *Inorg. Chem.* **1986**, *25*, 4131.

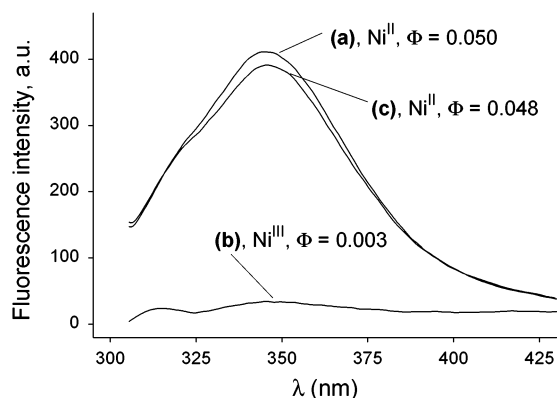


**Figure 6.** Emission spectra of  $[\text{Ni}^{\text{II}}(\mathbf{3})]^{2+}$  measured during controlled potential coulometry in aqueous 0.1 M  $\text{HClO}_4$ : prior to electrolysis (a); after electrolysis at 1.18 V (b); after electrolysis at 0.68 V (c).  $\lambda_{\text{exc}}$ : 280 nm.

We have now to establish through which intramolecular mechanism the  $\text{Ni}^{\text{III}}$  state is able to quench the nearby excited fluorophore. Such an assessment was carried out by measuring the emission spectra of the solutions of both the  $\text{Ni}^{\text{II}}$  and the  $\text{Ni}^{\text{III}}$  complexes (obtained through electrolysis), at room temperature and when frozen at 77 K. Butyronitrile (BuCN) was chosen as a solvent, because, on freezing, it does not crystallize, but forms a transparent glass (thus allowing the measurement of emission spectra). For instance, in the case of the macrocycle **2**, we observed that, at room temperature, the emission intensity at  $\lambda_{\text{max}} = 324$  nm of the  $\text{Ni}^{\text{II}}$  complex is at least 100 times higher than that of the  $\text{Ni}^{\text{III}}$  species. On the other hand, the BuCN solution frozen at the liquid nitrogen temperature of both  $\text{Ni}^{\text{II}}$  and  $\text{Ni}^{\text{III}}$  complexes shows emission bands, centered at  $\lambda_{\text{max}} = 315$  nm, which exhibit nearly the same intensity. If the frozen solutions are allowed to warm back to room temperature, a fluorescence quenching is again observed for the  $\text{Ni}^{\text{III}}$  complex since the emission intensity displayed by its BuCN solution is again much lower (by about 100 times) than that corresponding to the  $\text{Ni}^{\text{II}}$  complex.

In other words, freezing of the  $\text{Ni}^{\text{III}}$  complex solution makes fluorescence revive. With the exception of few examples of ultrafast eT processes,<sup>29</sup> the reviving of fluorescence in frozen solution is generally expected when an electron transfer (eT) rather than an energy transfer (ET) process is responsible for the fluorescence quenching at room temperature.

In particular, the eT process involves a drastic rearrangement of the system of electrical charges: following the eT process, the positive charge on the metal center is reduced, while a positive charge is formed on the appended donor group. A substantial reorganization of the molecules of the polar solvent (BuCN, in the present case) must accompany the process of electrical charge rearrangement. However, at the liquid nitrogen temperature, the solvent molecules are immobilized, a situation which prevents the occurrence of the electron transfer process from the excited fluorophore to  $\text{Ni}^{\text{III}}$ . Thus, the excited fluorophore releases photonic

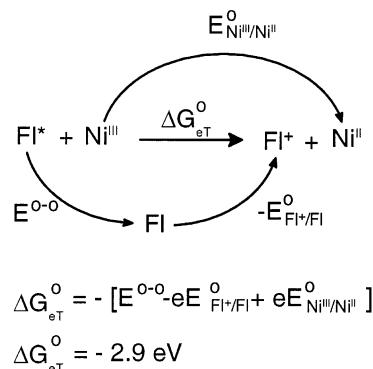


**Figure 7.** Thermodynamic cycle for evaluating the free energy change  $\Delta G_{\text{eT}}^{\circ}$  associated with the intramolecular photoinduced electron transfer in the nickel(III) complex of **3**.  $E^{0-0} = 3.6$  eV;  $E^{\circ}(\text{FI}^+/\text{FI}) = 1.43$  V (irreversible peak);  $E^{\circ}(\text{Ni}^{\text{III}}/\text{Ni}^{\text{II}}) = 0.73$  V. The Coulombic term has been considered negligible under the present circumstances. A similar cycle can be drawn for the complex  $[\text{Ni}^{\text{II}}(\mathbf{2})]^{2+}$ .

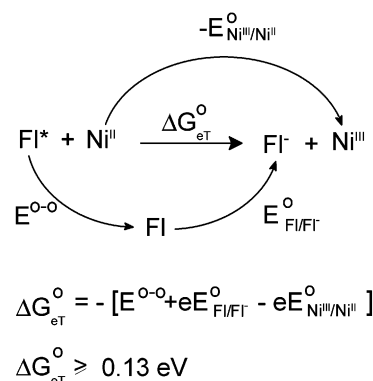


**Figure 8.** Thermodynamic cycle for evaluating the free energy change  $\Delta G_{\text{eT}}^{\circ}$  associated with the intramolecular photoinduced electron transfer in the  $[\text{Ni}^{\text{II}}(\mathbf{3})]^{2+}$  complex.  $E^{0-0} = 3.6$  eV;  $E^{\circ}(\text{FI}/\text{FI}^-) \leq 3.0$  V, since no peaks were observed in the cathodic scan in voltammetry experiments until solvent discharge;  $E^{\circ}(\text{Ni}^{\text{III}}/\text{Ni}^{\text{II}}) = 0.73$  V. The Coulombic term has been considered negligible under the present circumstances. A similar cycle can be drawn for the complex  $[\text{Ni}^{\text{II}}(\mathbf{2})]^{2+}$ .

energy in its normal radiative mode and, in a frozen situation, fluorescence is revived. It has to be noted that the electronic energy transfer mechanism, according to the Dexter mechanism, does not involve any electrical rearrangement and reorganization of the solvation sphere: thus, it takes place both in the liquid and in the glass, quenching fluorescence both at room temperature and at 77 K.

The occurrence of a fluorophore-to- $\text{Ni}^{\text{III}}$  electron transfer process can be accounted for also on a thermodynamic basis. In particular, the free energy change,  $\Delta G_{\text{eT}}^{\circ}$ , associated with the eT process can be calculated through the thermodynamic cycle (illustrated in Figure 7 for  $[\text{Ni}^{\text{III}}(\mathbf{3})]^{3+}$ ), by combining the appropriate photophysical and electrochemical quantities:  $E^{0-0}$ , the photonic energy, which is obtained from the emission spectrum;  $E^{\circ}(\text{Ni}^{\text{III}}/\text{Ni}^{\text{II}})$  and  $E^{\circ}(\text{FI}^+/\text{FI})$ , which refer to the standard electrode potentials for the redox change involving the macrocyclic complex and the fluorogenic substituent FI respectively, and are obtained from the corresponding  $E_{1/2}$  values. Calculated  $\Delta G_{\text{eT}}^{\circ}$  values are all distinctly negative (system **2**,  $-3.0$  eV; **3**,  $-2.9$  eV), and account for the quenching of fluorescence occurring in the  $\text{Ni}^{\text{III}}$  derivatives, through an eT mechanism.

(29) Wasielewski, M. R.; O'Neil, M. P.; Gosztola, D.; Niemczyk, M. P.; Svec, W. A. *Pure Appl. Chem.* **1992**, *64*, 1325.



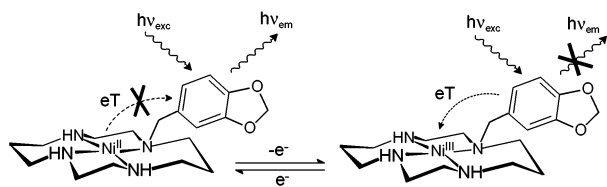


**Figure 9.** The mechanism of the redox switching of fluorescence in the two-component system  $[\text{Ni}^{\text{II}}(\mathbf{2})]^{2+}$ : the oxidized form induces a fluorophore-to- $\text{Ni}^{\text{III}}$  eT process and causes fluorescence quenching; in the reduced form, the  $\text{Ni}^{\text{II}}$ -to-fluorophore eT process is thermodynamically disfavored. A similar mechanism operates in the  $[\text{Ni}^{\text{II}}(\mathbf{3})]^{2+}$  system.

The thermodynamic approach can also explain why no fluorescence quenching is observed when the system is in the  $\text{Ni}^{\text{II}}$  state. In fact, the possible eT process (from  $\text{Ni}^{\text{II}}$  to the excited fluorophore) is characterized by a positive value of  $\Delta G^{\circ}_{\text{eT}}$  (system **2**,  $\geq 0.05$  eV; **3**,  $\geq 0.13$  eV), as calculated from the appropriate thermodynamic cycle like the one depicted in Figure 8 for the complex  $[\text{Ni}^{\text{II}}(\mathbf{3})]^{2+}$ .

The mechanism of the fluorescence switching process for the  $[\text{Ni}^{\text{II}}(\mathbf{2})]^{2+}$  system is pictorially illustrated in Figure 9.

## Conclusions

Molecular switches of fluorescence can be constructed by covalently linking a fluorogenic fragment to a redox active subunit. Subunits containing a metal center can provide two consecutive oxidation states of comparable stability and connected by a one-electron fast and reversible redox change. Hopefully, the two states should interact differently with the

nearby excited fluorophore. This is the case of the  $\text{Ni}^{\text{III}}/\text{Ni}^{\text{II}}$  couple in the systems investigated in this work: the oxidized form,  $\text{Ni}^{\text{III}}$ , is capable of establishing an electron transfer process with the charge transfer excited state,  $\text{Fl}^*$  (i.e., from  $\text{Fl}^*$  to  $\text{Ni}^{\text{III}}$ , fluorescence OFF). On the other hand, the occurrence of an eT process involving the reduced state (i.e., from  $\text{Ni}^{\text{II}}$  to  $\text{Fl}^*$ ) is prevented by the very endoergic contribution associated with the reduction of the fluorogenic fragment (fluorescence ON).

Previously reported  $\text{Ni}^{\text{III}}/\text{Ni}^{\text{II}}$  based switches of fluorescence contained polyaromatic fluorophores with a  $\pi-\pi^*$  excited state (e.g., anthracene). The use of aromatic fluorophores containing donor substituents, as described in this work, provides a charge transfer excited state (with a relatively high value of the photonic energy) and produces water soluble systems, an important new feature.

**Acknowledgment.** This work has been supported by the Italian Ministry of University and Research (MIUR, Progetto “Dispositivi Supramolecolari”) and the European Commission (RTN Molecular Level Devices and Machines). We thank “Centro di Studi per la Cristallografia e la Cristallografia” (CNR), Pavia, for providing X-ray crystallographic facilities.

**Supporting Information Available:** Crystallographic data in CIF format. This material is available free of charge via the Internet at <http://pubs.acs.org>.

IC025826B